Supporting Information

Contents:

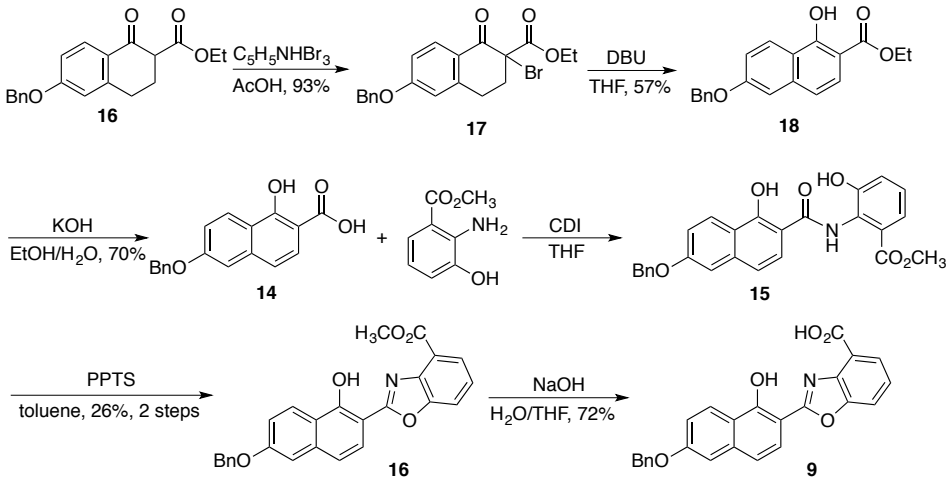

Scheme S1: Synthesis of Compound **9**.

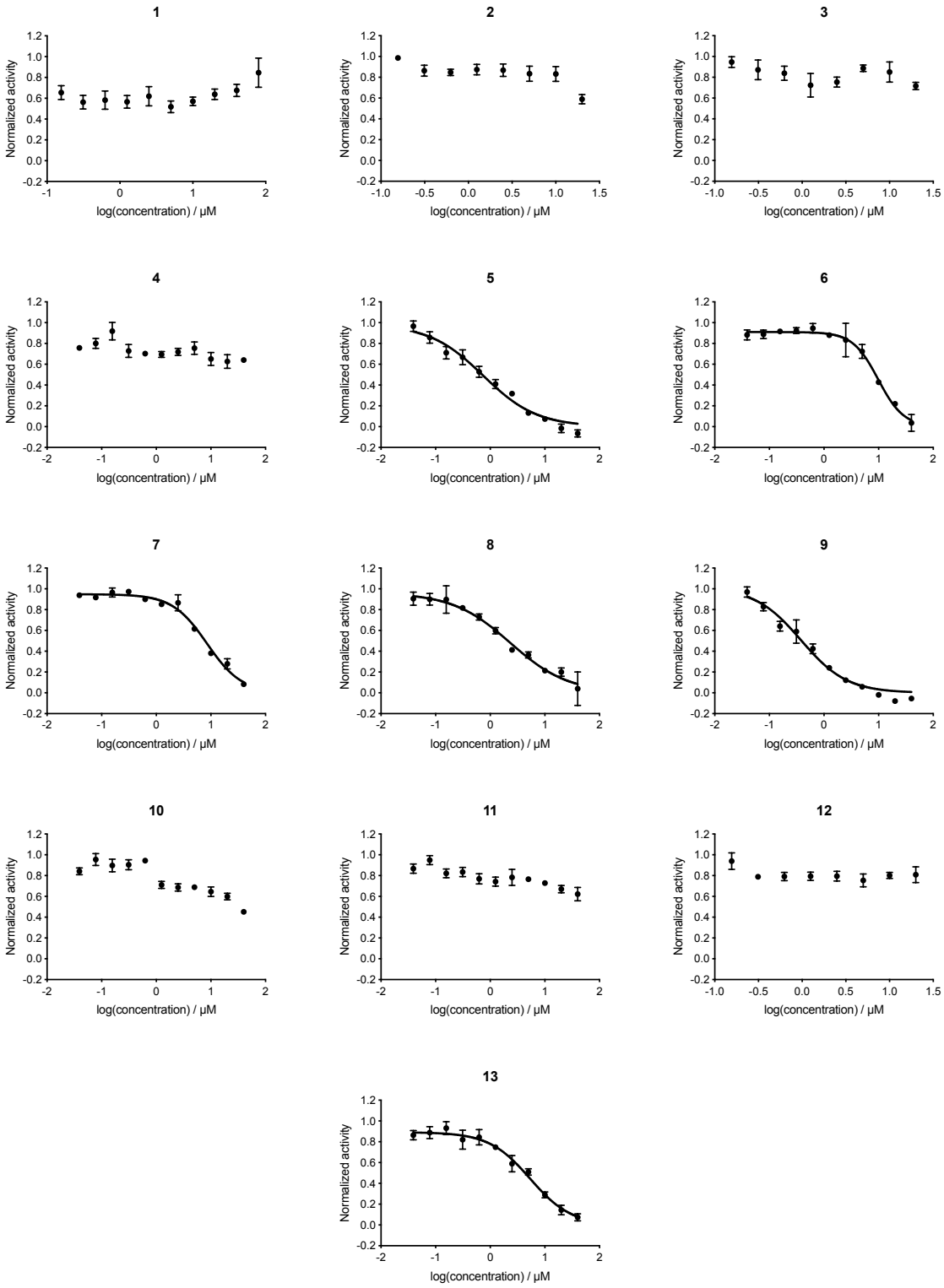

Figure S1: Inhibition curves used to determine IC_{50} values of compounds. Compounds were incubated with 1 nM NDM-1 in HEPES (50 mM, pH 7.2) for 10 min before addition of 20 μM nitrocefin. Absorbance at 492 nm was monitored over 30 min as a measure of NDM-1 activity.

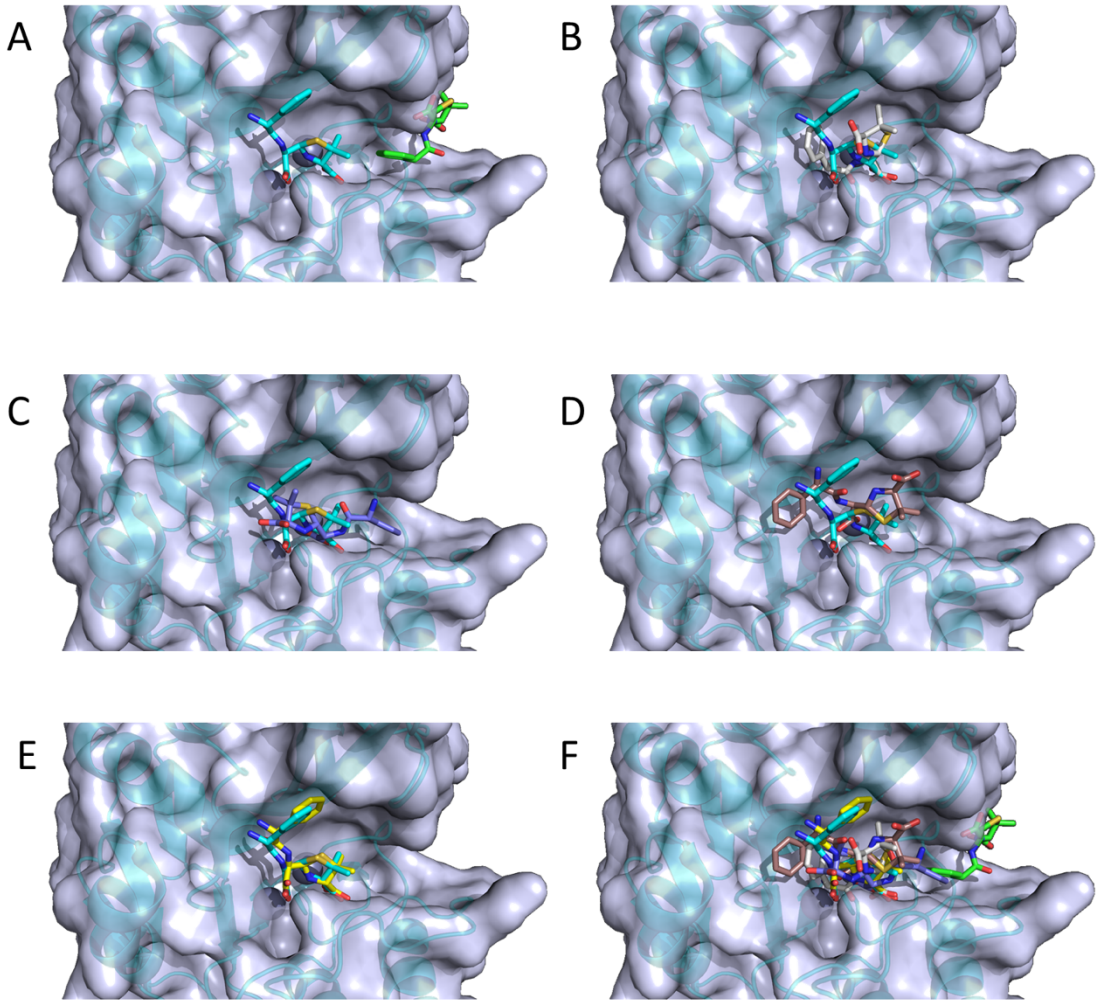

Figure S2: Re-docking of hydrolyzed ampicillin to NDM-1 5ZGR. Each panel shows the lowest cluster energy solution for A) Autodock Vina, B) AD4.2, no charge on zinc, C) AD4.2 with 2+ charge on zinc, D) AD4.2 zinc charge diffusion, E) Autodock4Zn, and F) all methods. In each panel the position of the hydrolyzed ampicillin is shown in cyan. Autodock4Zn showed the closest agreement with the crystal structure with only minor changes to the position of the phenyl within the active site pocket. The protein backbone is shown as a cyan ribbon oriented with the N-terminus at the top and C-terminus at the bottom of each and the active site cleft facing forward. The two zinc ions in the 5ZGR active site are shown as grey spheres. Stick models of the hydrolyzed ampicillin are colored by element.

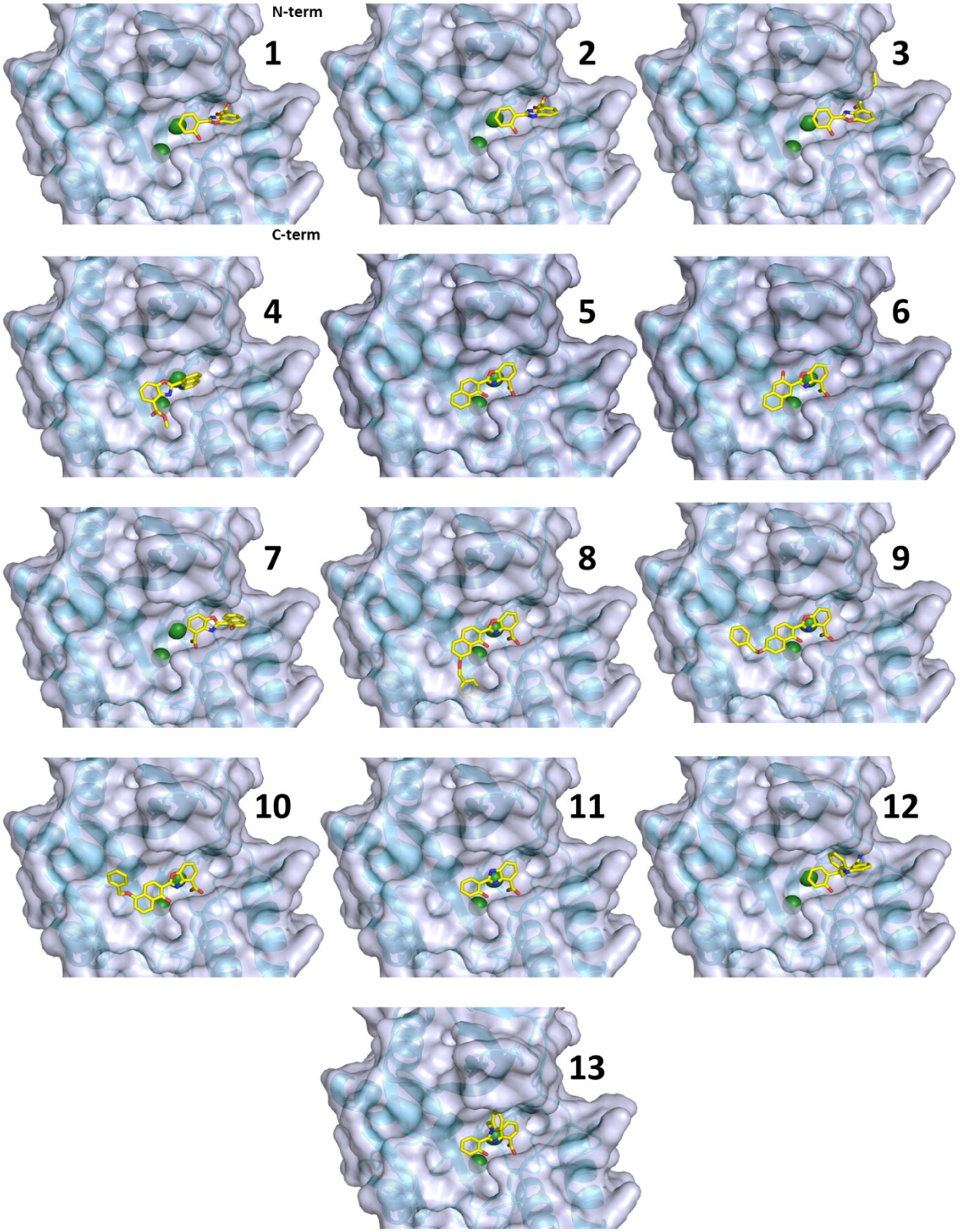

Figure S3: Docked poses (lowest energy pose of the lowest energy cluster) of each compound to the 5ZGR X-ray crystal structure. The protein backbone is shown as a cyan ribbon model with the N-terminus at the top and C-terminus at the bottom of each and the active site cleft facing forward. The two zinc ions in the 5ZGR active site are shown as green spheres. Compounds are colored by element type with carbons shown in yellow.

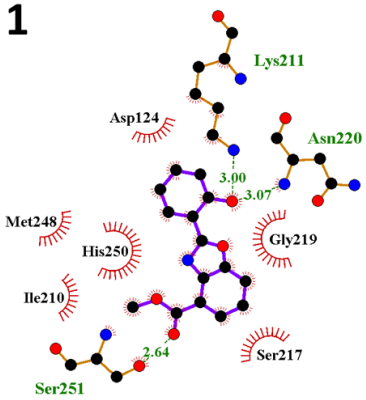
1
Lys211
Asp124
Asn220
3.00
3.07
Met248
His250
Gly219
Ile210
2.64
Ser217
Ser251

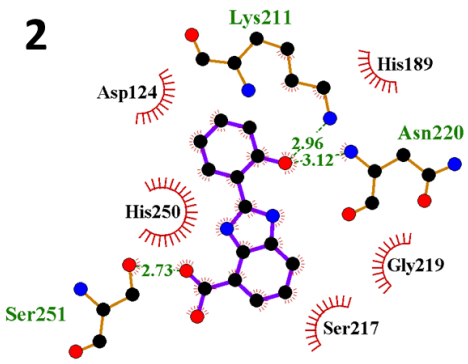
2
Lys211
His189
Asp124
Asn220
2.96
3.12
His250
Gly219
2.73
Ser251
Ser217

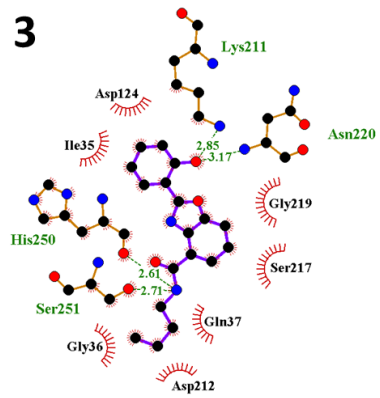
3
Lys211
Asp124
Asn220
Ile35
2.85
3.17
Gly219
His250
Ser217
2.61
2.71
Ser251
Gln37
Gly36
Asp212

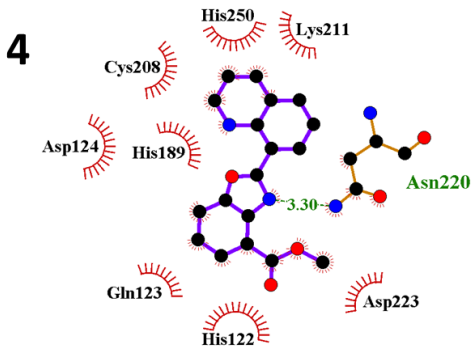
4
His250
Lys211
Cys208
Asp124
His189
Asn220
3.30
Gln123
Asp223
His122

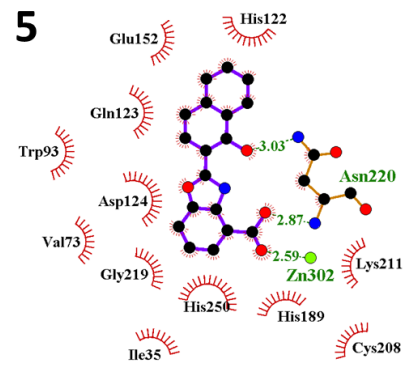
5
His122
Glu152
Gln123
Trp93
3.03
Asn220
Asp124
2.87
Val73
2.59
Lys211
Gly219
Zn302
His250
His189
Ile35
Cys208

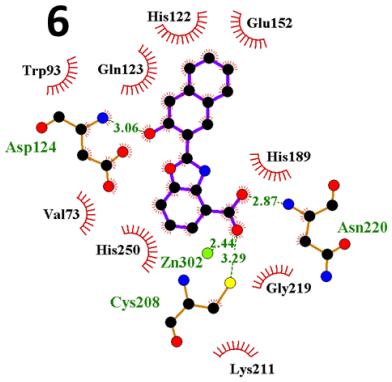
6
His122
Glu152
Trp93
Gln123
3.06
Asp124
His189
2.87
Val73
Asn220
His250
2.44
Zn302
3.29
Gly219
Cys208
Lys211

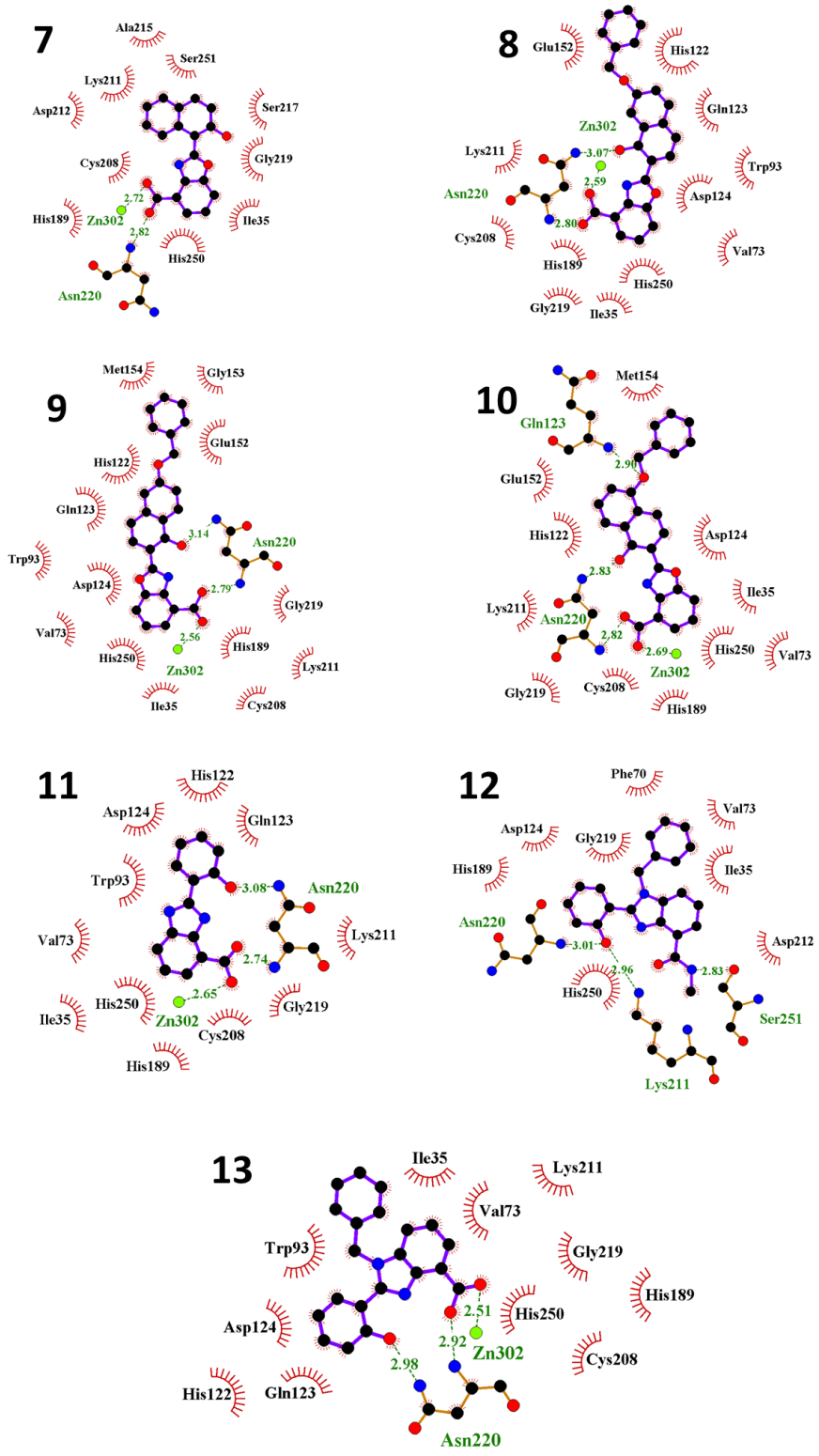

Figure S4: LigPlots generated for each docked compound. Compounds are shown with purple bonds, amino acid residues are shown with orange bonds. Hydrophobic interactions are indicated with residues labelled in black. Hydrogen bonds and bonding residues are shown and labelled in green.

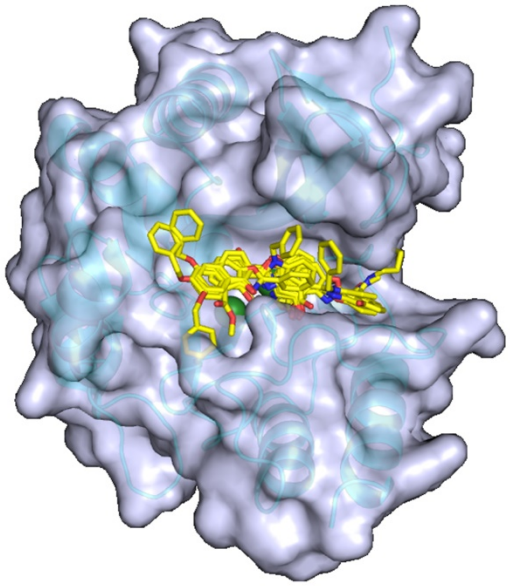

Figure S5: Overlay of all docked ligands to 5ZGR X-ray crystal structure active site.

Table S1: Interactions between compounds and NDM-1 residues from docked structures by LigPlot+.

Compound	H-bonding interactions	Hydrophobic interactions
1	Lys211, Asn220, Ser251	Asp124, Ile210, Ser217, Gly219, Met248, His250
2	Lys211, Asn220, Ser251	Asp124, His210, Ser217, Gly219, His250
3	Lys211, Asn220, His250, Ser251	Ile35, Gly36, Gln37, Asp124, Asp212, Ser217, Gly219
4	Asn220	His122, Gln123, Asp124, His189, Cys208, Lys211, Asp223
5	Asn220, Zn302	Ile35, Val73, Trp93, His122, Gln123, Asp124, Glu152, His189, Cys208, Lys211, Gly219, His250
6	Asp124, Cys208, Asn220, Zn302	Val73, Trp93, His122, Gln123, Glu152, His189, Lys211, Gly219, His250
7	Ans220, Zn302	Ile35, His189, Cys208, Lys211, Asp212, Ala215, Ser217, Gly219, His250, Ser251
8	Asn220, Zn302	Ile35, Val73, Trp93, His122, Gln123, Asp124, Glu152, His189, Cys208, Lys211, Gly219, His250
9	Asn220, Zn302	Ile35, Val73, Trp93, His122, Gln123, Asp124, Glu152, Gly153, Met154, His189, Cys208, Lys211, Gly219, His250
10	Asn220, Zn302	Ile35, Val73, His122, Asp124, Glu152, Met154, His189, Cys208, Lys211, Gly219, His250
11	Asn220, Zn302	Ile35, Val73, Trp93, His122, Gln123, Asp124, His189, Cys208, Lys211, Gly219, His250
12	Lys211, Asn220, Ser251	Ile35, Phe70, Val73, Asp124, His189, Asp212, Gly219, His250
13	Asn220, Zn302	Ile35, Val73, Trp93, His122, Gln123, Asp124, His189, Cys208, Lys211, Gly219, His250

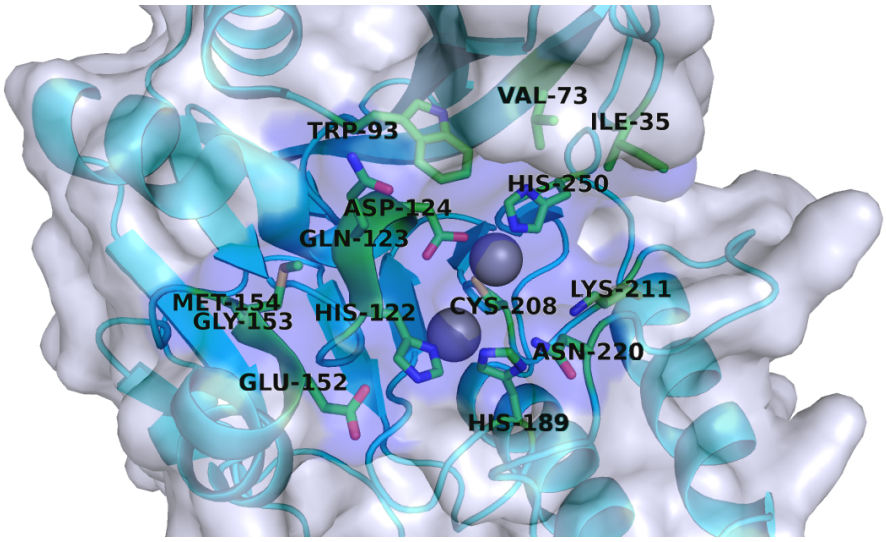

Figure S6: Highlighted residues in the active site pocket of 5ZGR NDM-1 involved in binding **9** from docking analysis. Identified residues are labelled, with the side-chain shown as sticks in green, and the surface shown in blue. Zn1 is coordinated by His122, His 189 and His 120 (not shown), while Zn2 is coordinated by Asp124, His250 and Cys208.

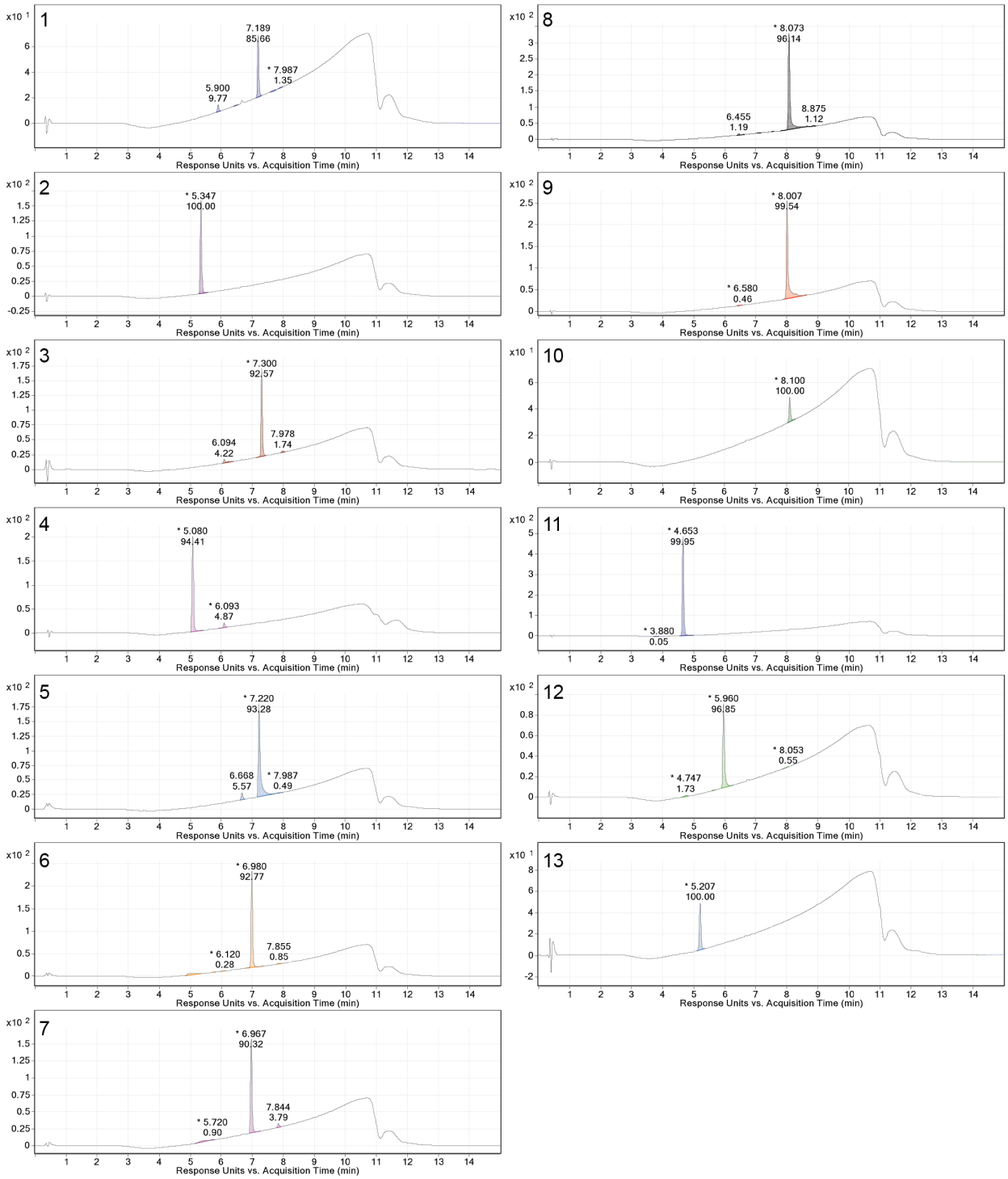

Figure S7: HPLC traces of compounds **1**–**13**. UV chromatograms at 254 nm are shown. Peaks are labeled with the integral and percentage relative to all peaks. For all compounds, the largest peak corresponded to the expected mass (see HR-MS in the Experimental section).

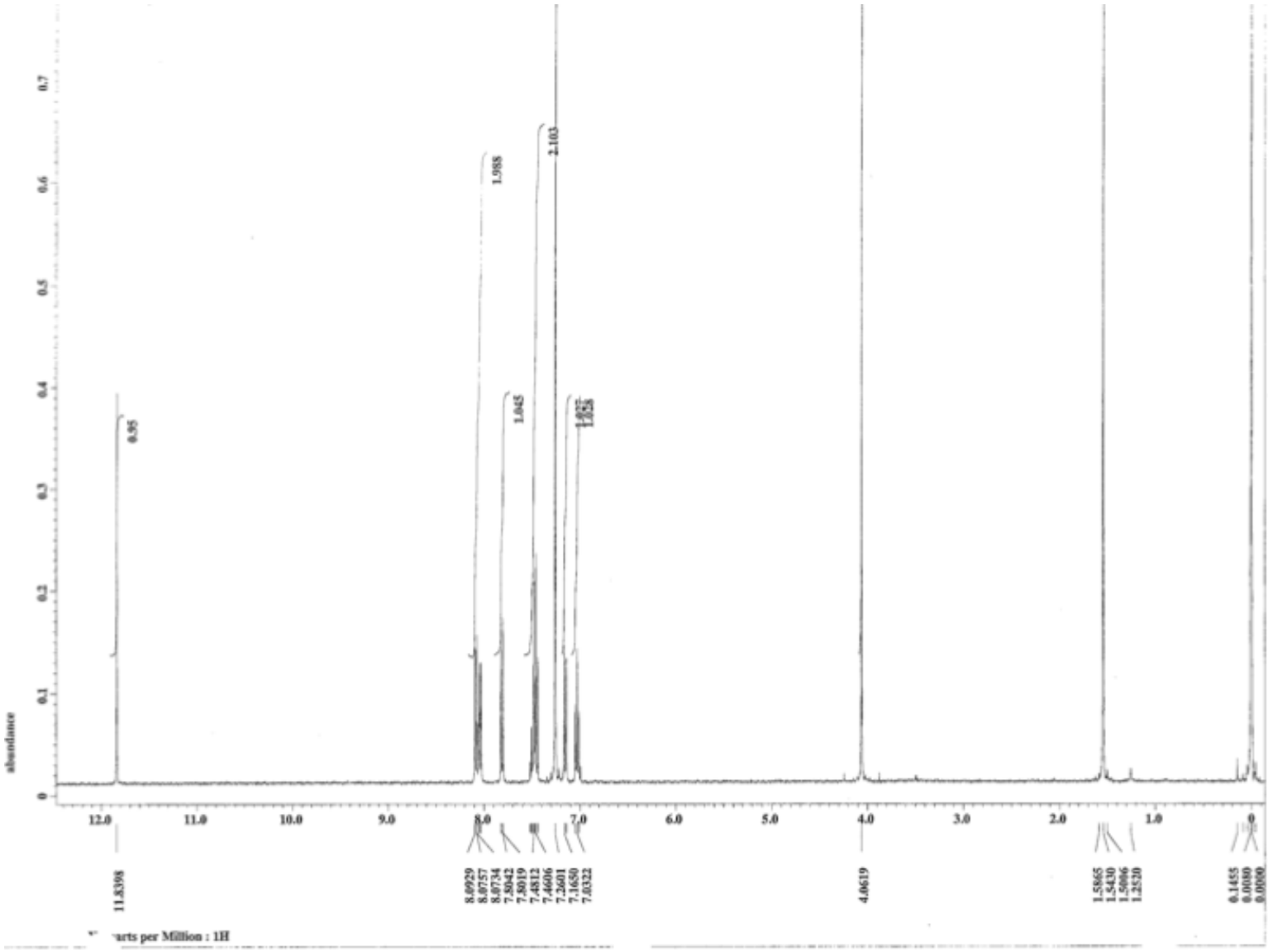

Figure S8. ^{1}H NMR spectrum of compound **1** taken in $CDCl_3$. Residual peaks at 7.26 and 1.54 are due to $CHCl_3$ and water, respectively. Estimate of purity: 97%.

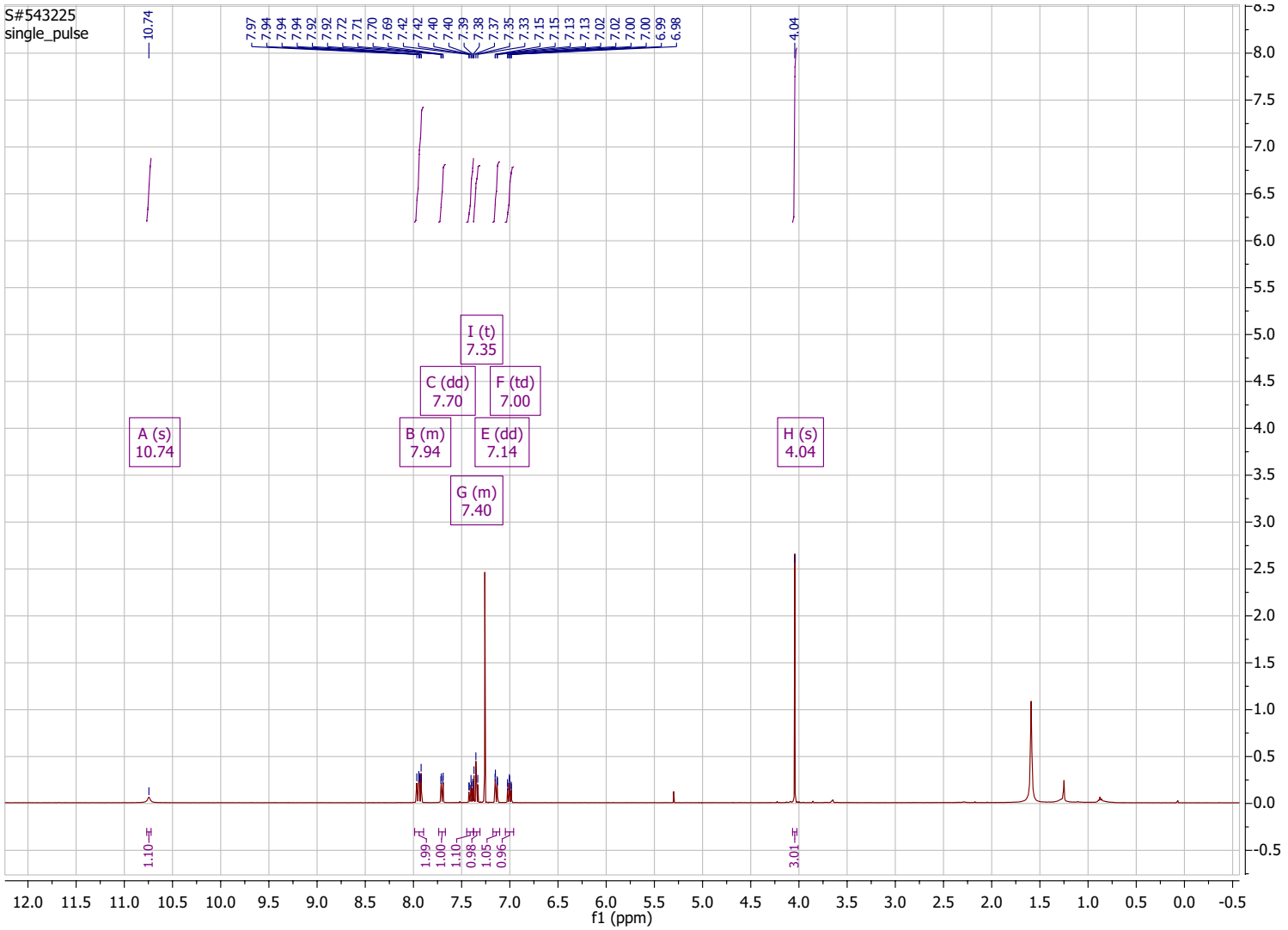

Figure S9. ^{1}H NMR spectrum of compound **2** taken in $CDCl_3$. Residual peaks at 7.26 and 1.54 are due to $CHCl_3$ and water, respectively. Estimate of purity: 97%.

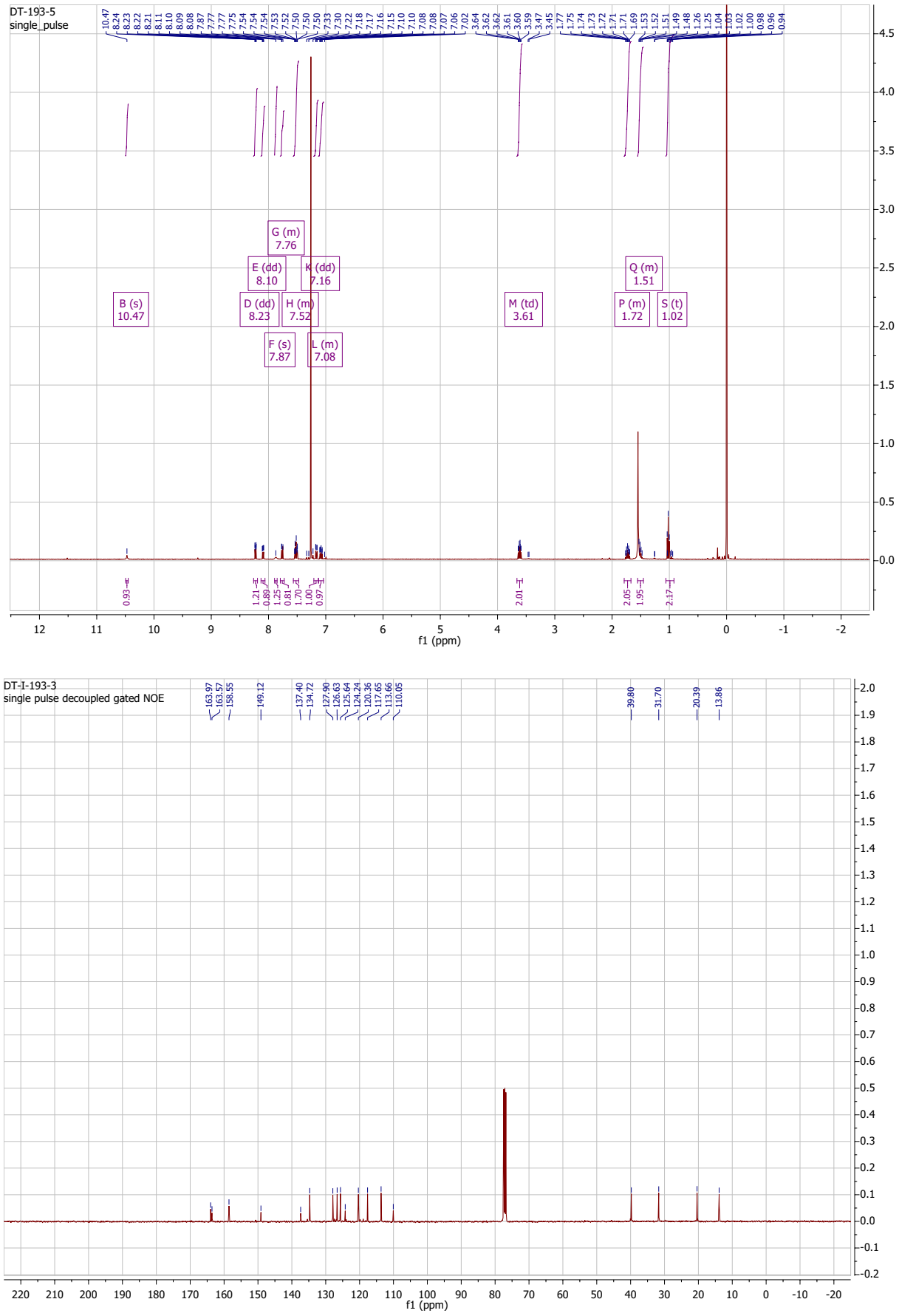

Figure S10. ^{1}H (top) and ^{13}C NMR (bottom) spectra of compound **3** taken in $CDCl_3$. Residual peaks in the ^{1}H spectrum at 7.26 and 1.54 are due to $CHCl_3$ and water, respectively. Estimate of purity: 95%.

Figure S11. ^{1}H (top) and ^{13}C NMR (bottom) spectra of compound **4** in $CDCl_3$. The residual peak in the ^{1}H spectrum at 7.26 is due to $CHCl_3$. Estimate of purity: 97%.

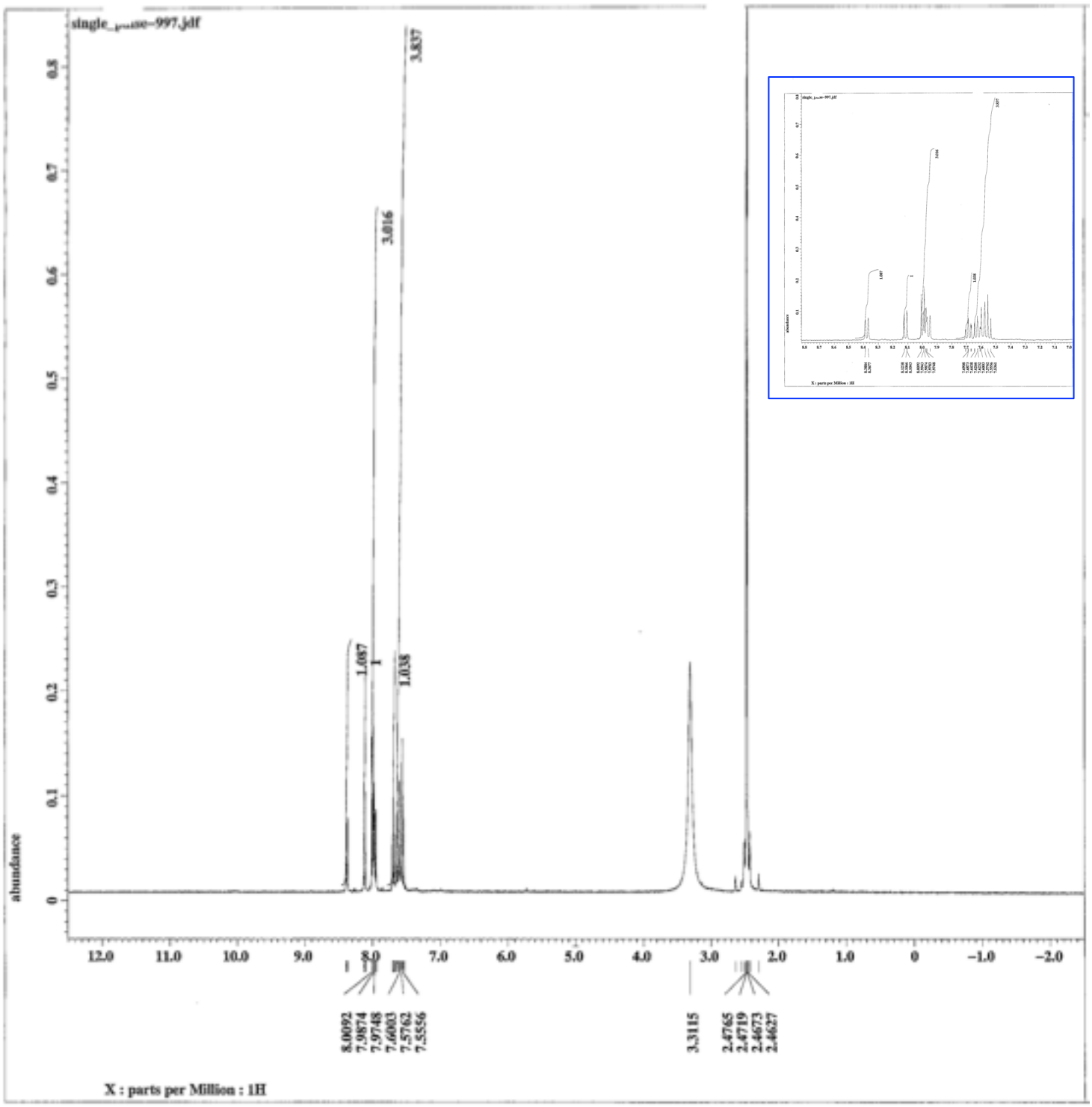

Figure S12. ^{1}H NMR spectrum of compound **5** in D-6 DMSO; inset shows aromatic region zoomed in. Residual peaks at 3.31 and 2.47 are due to water and DMSO. Estimate of purity: 95%.

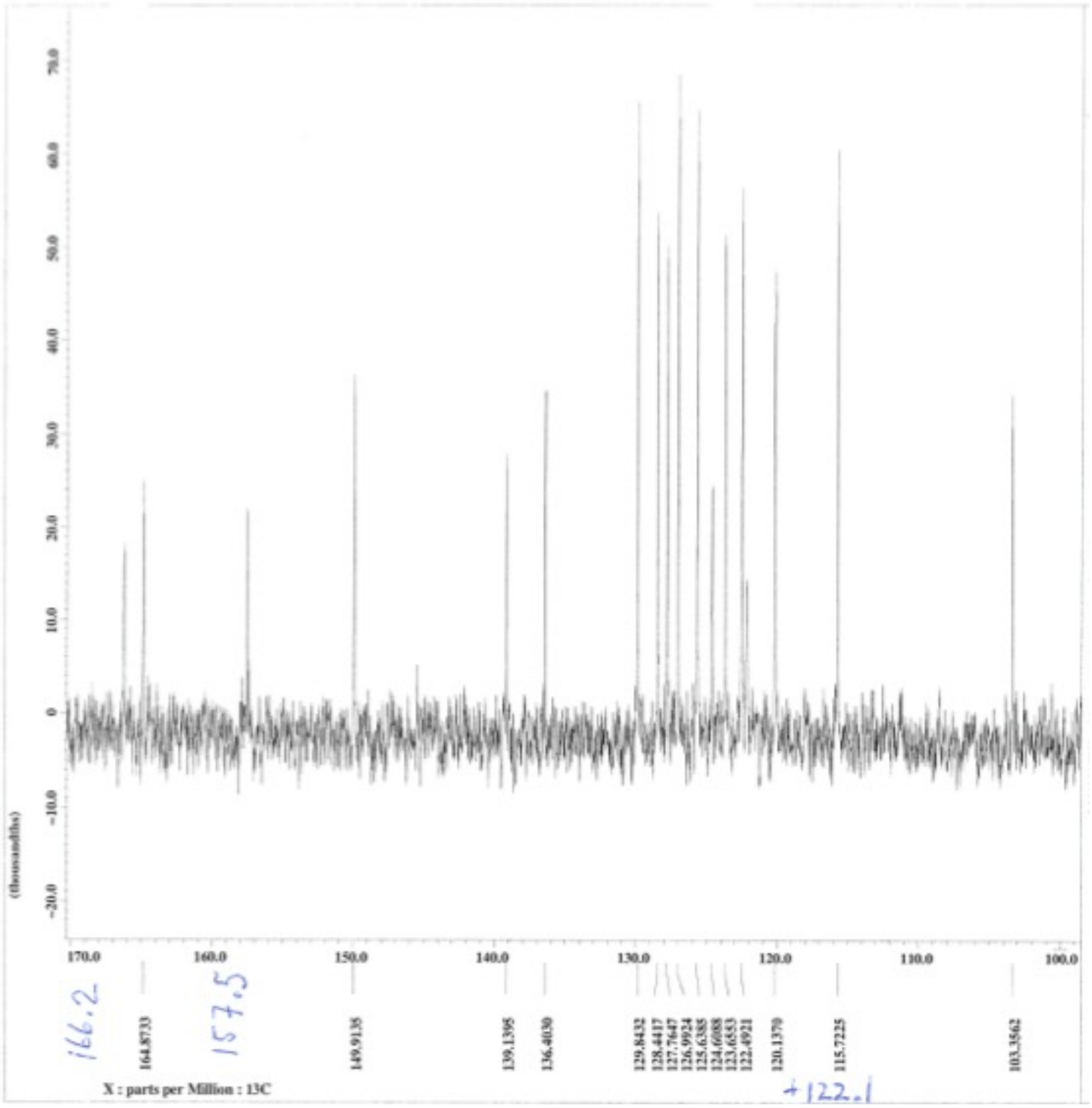

Figure S13. ^{13}C NMR spectrum of compound **5** in D-6 DMSO.

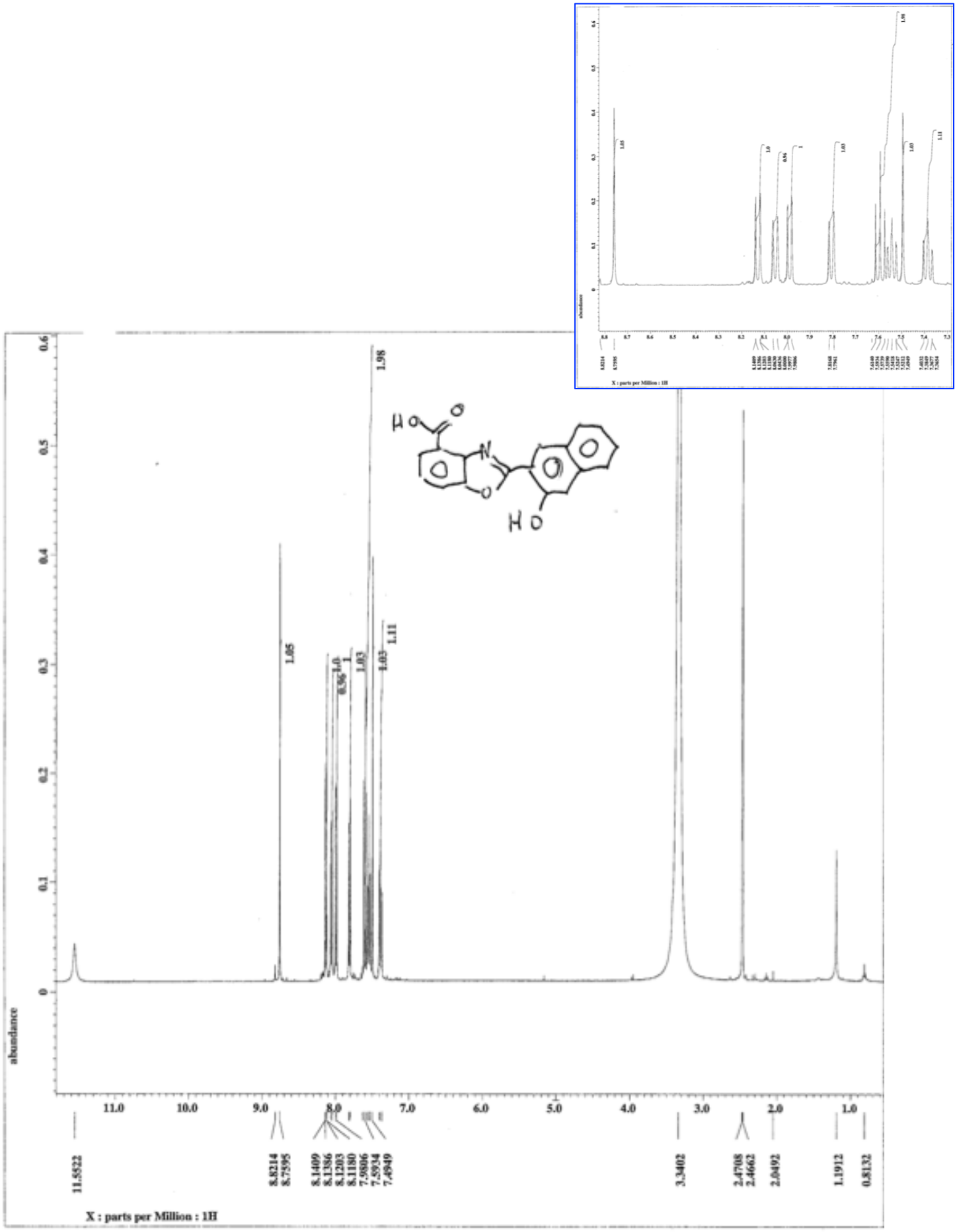

Figure S14. ^{1}H NMR spectrum of compound **6** in D6-DMSO; inset shows aromatic region zoomed in. Residual peaks at 3.34 and 2.47 are due to water and DMSO. Estimate of purity: 95%.

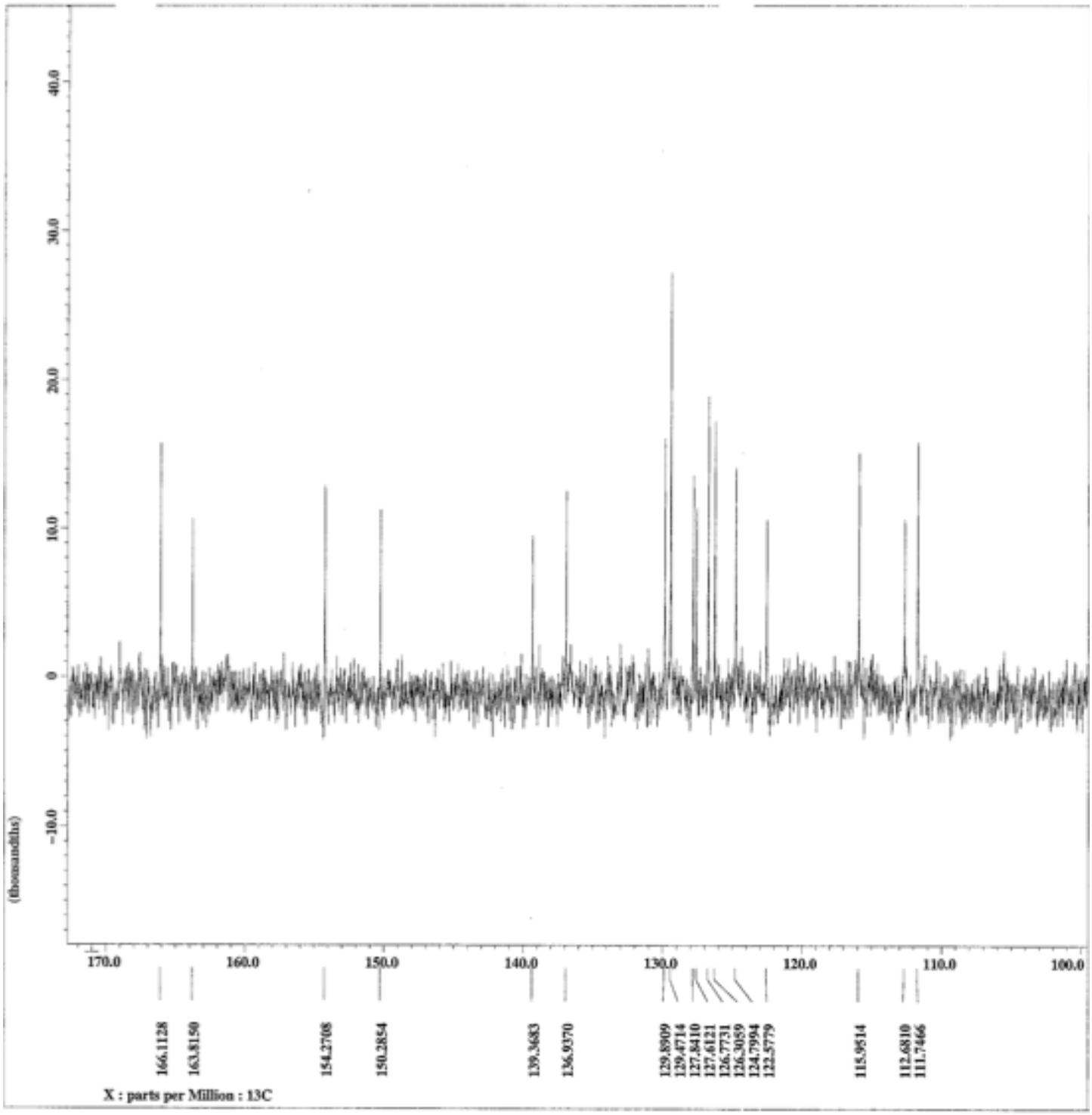

Figure S15. ^{13}C NMR spectra of compound **6** in D6-DMSO.

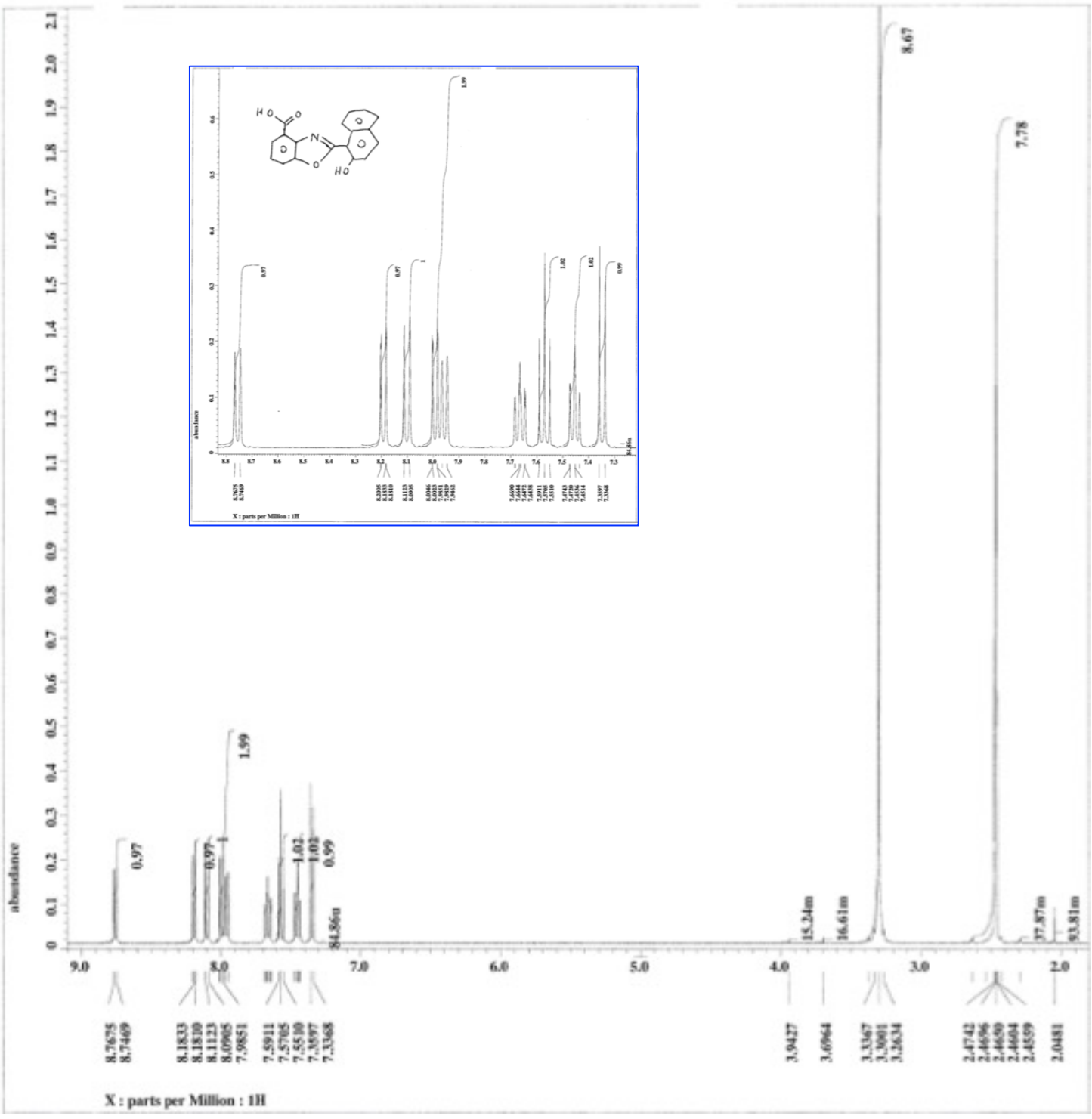

Figure S16. [1]H NMR spectrum of compound **7** in D6-DMSO; inset shows aromatic region zoomed in. Residual peaks at 3.30 and 2.47 are due to water and DMSO. Estimate of purity: 97%.

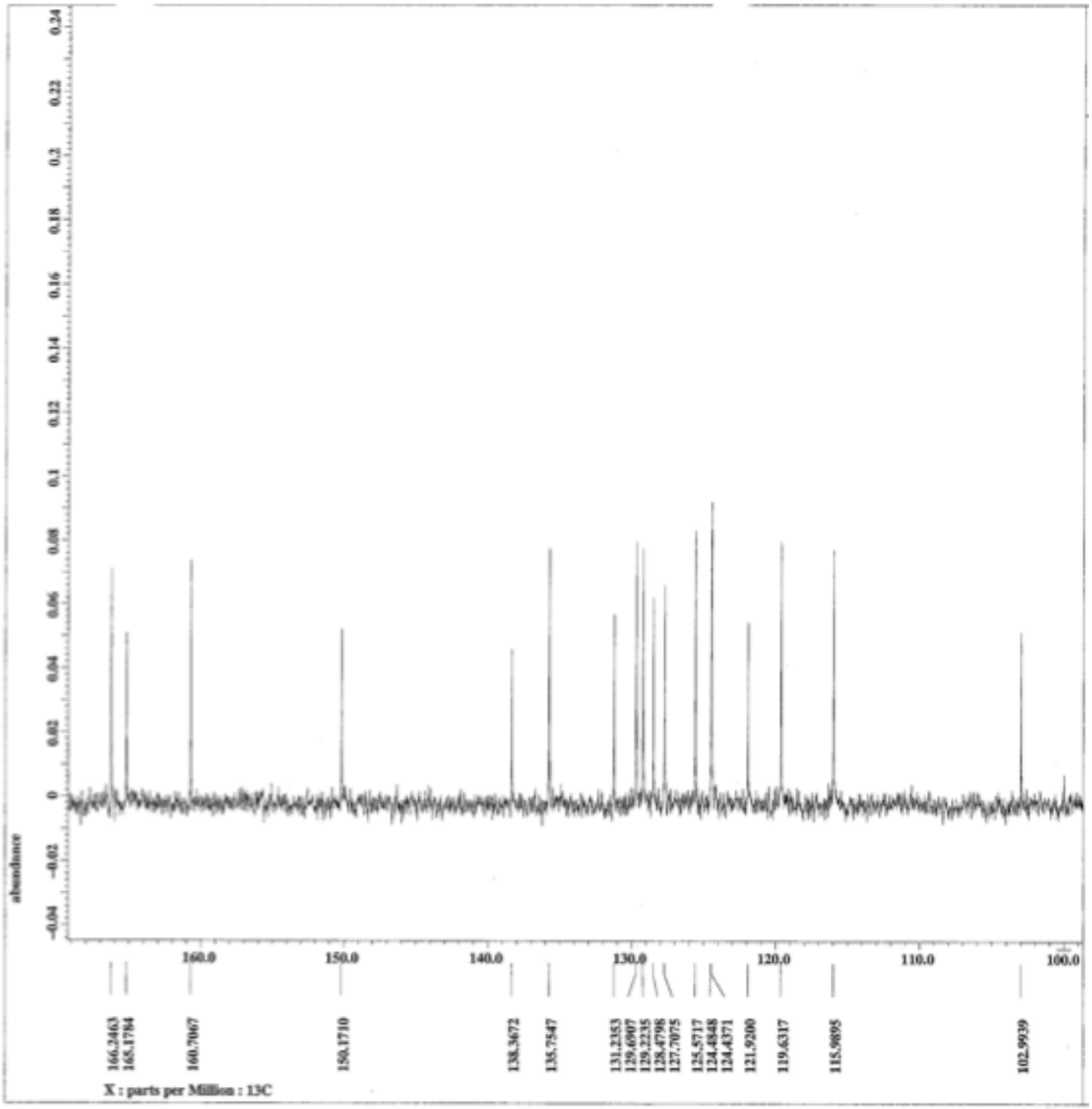

Figure S17. ^{13}C NMR spectra of compound **7** in D6-DMSO.

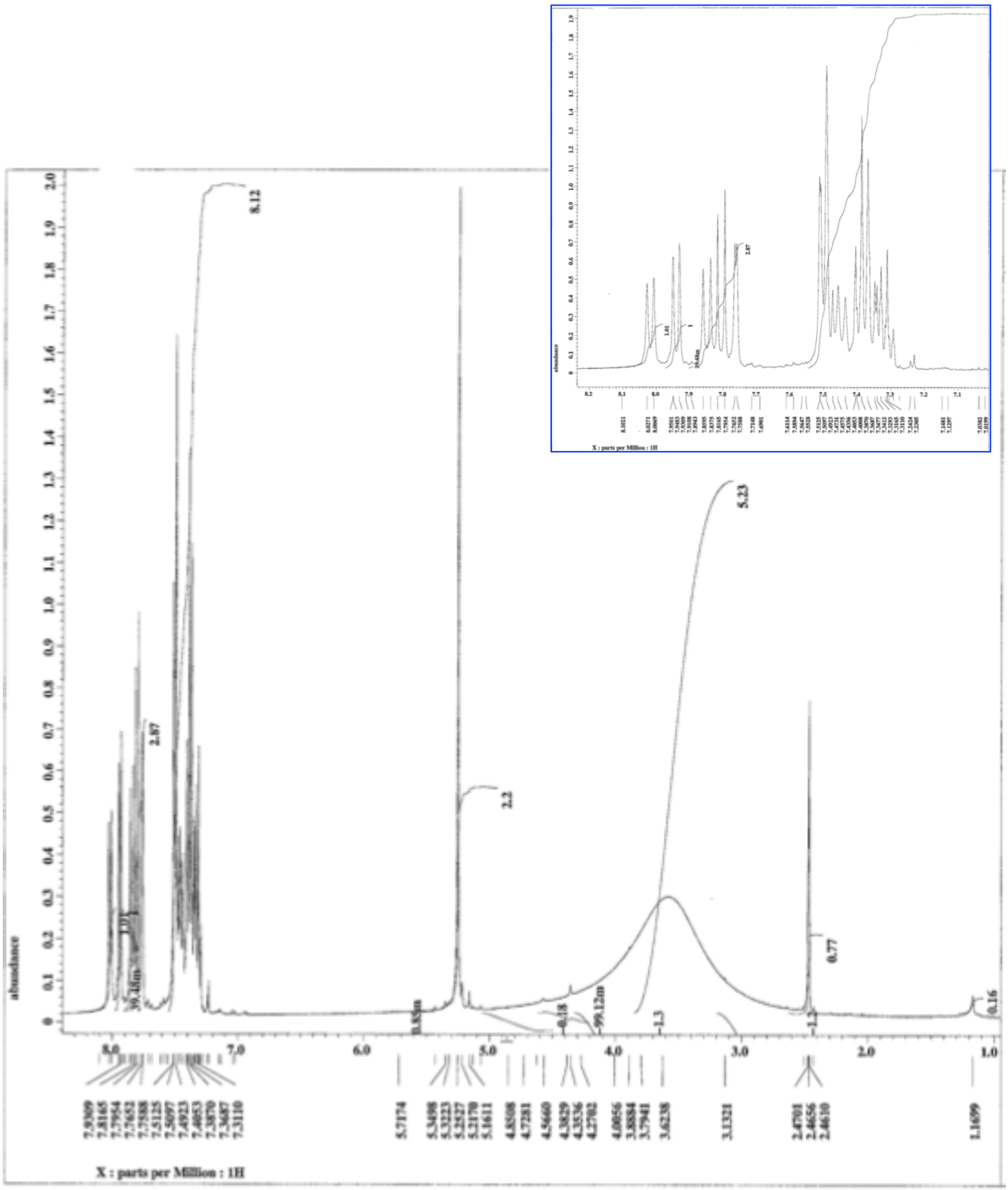

Figure S18. ^{1}H NMR spectrum of compound **8** in D6-DMSO; inset shows aromatic region zoomed in. Residual peaks at 3.62 and 2.47 are due to water and DMSO. Estimate of purity: 95%.

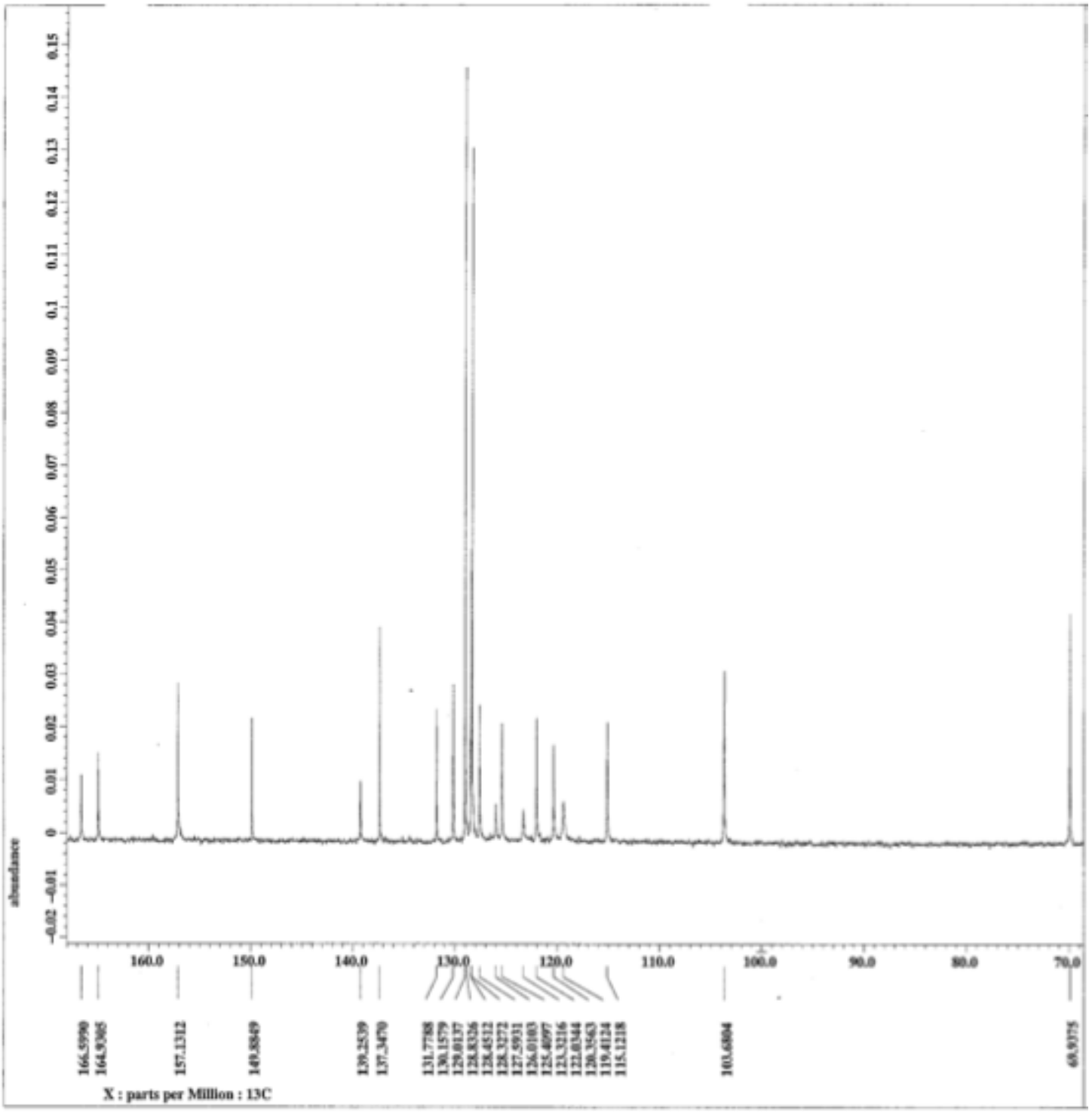

Figure S19. ^{13}C NMR spectrum of compound **8** in D6-DMSO**.**

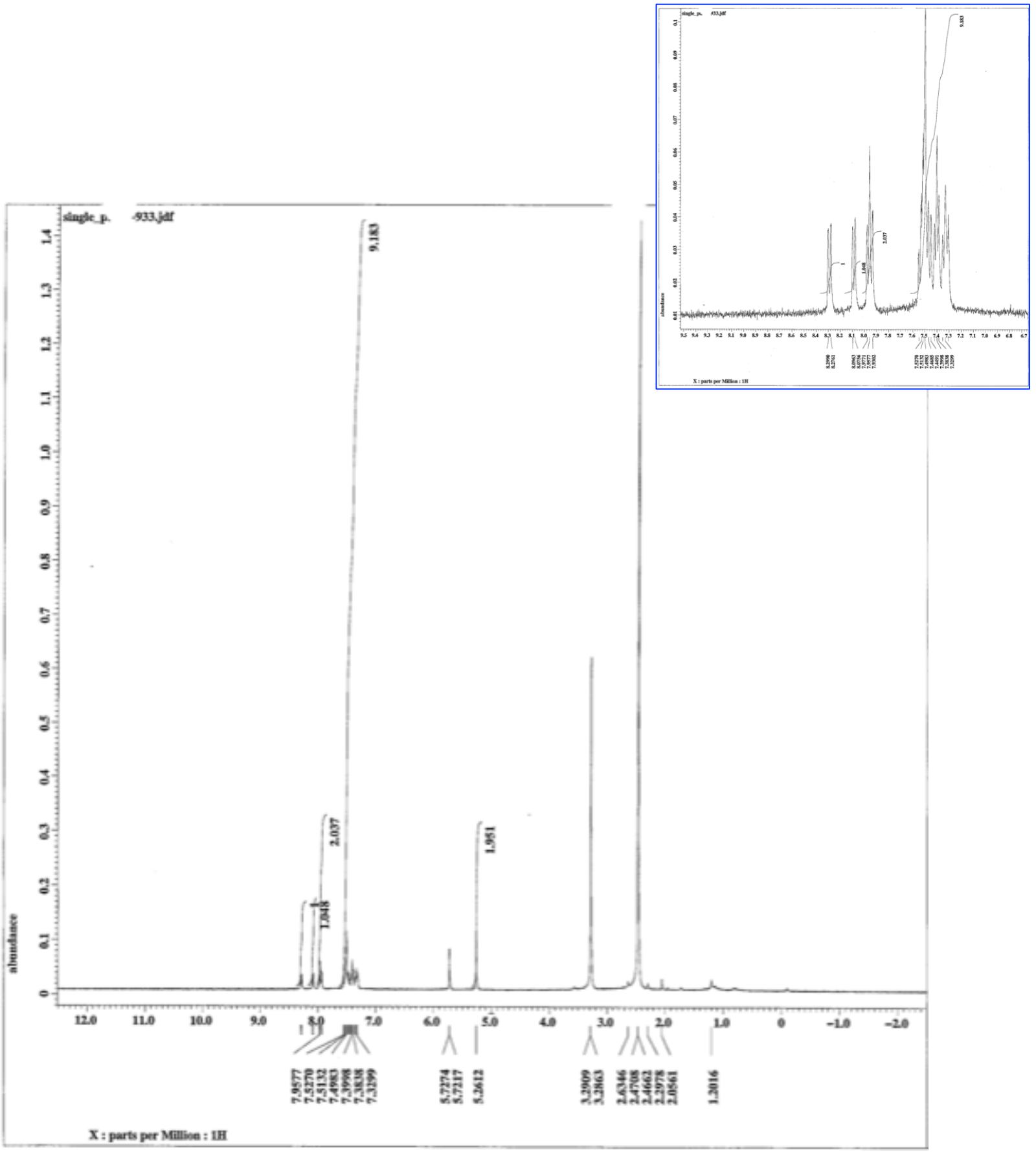

Figure S20. ^{1}H NMR spectrum of compound **9** in D6-DMSO; inset shows aromatic region zoomed in. Residual peaks at 5.72, 3.30 and 2.47 are due to CH_2Cl_2, water, and DMSO, respectively. Estimate of purity: 95%.

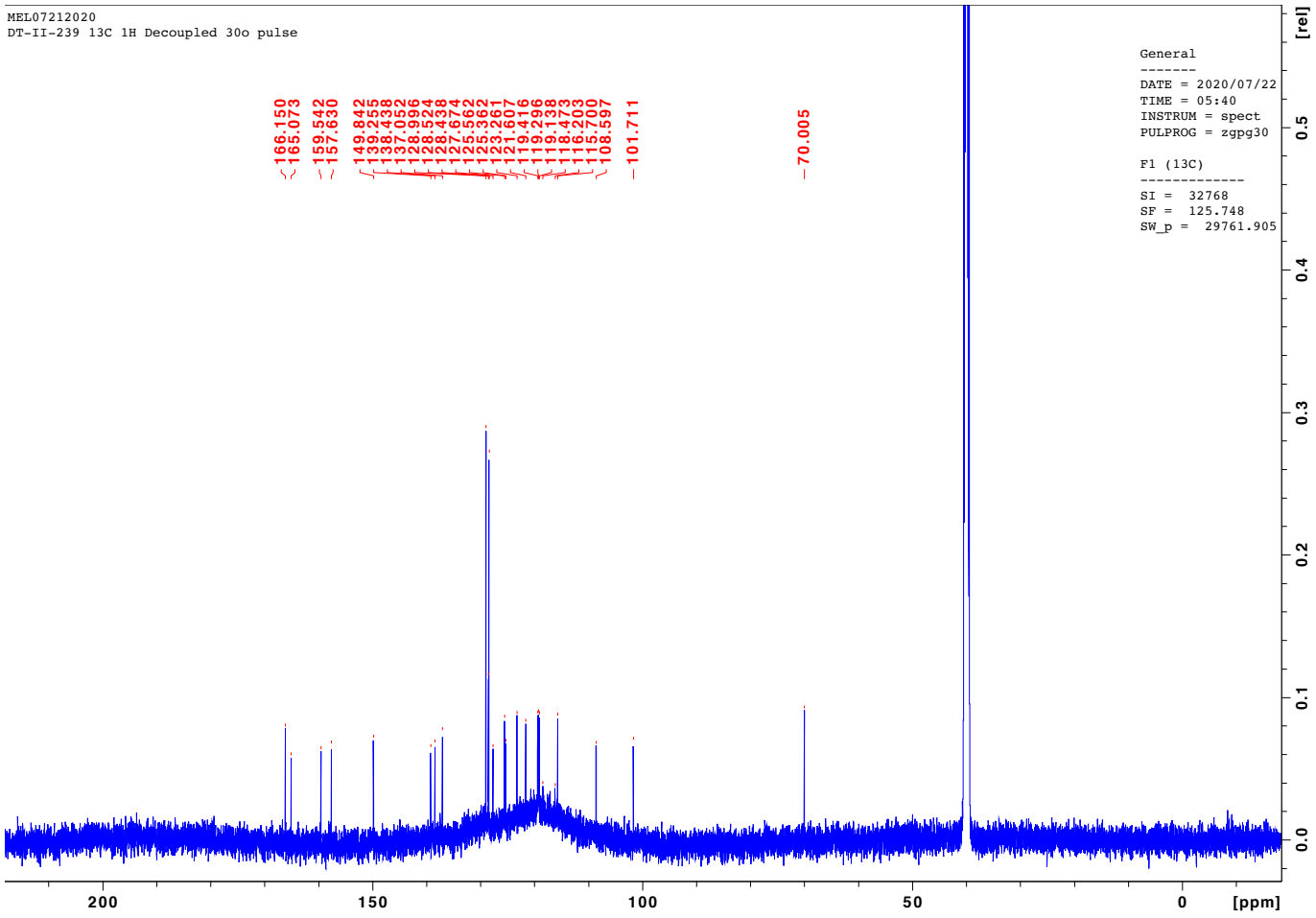

Figure S21. ^{13}C NMR spectrum of compound **9** in D6-DMSO**.**

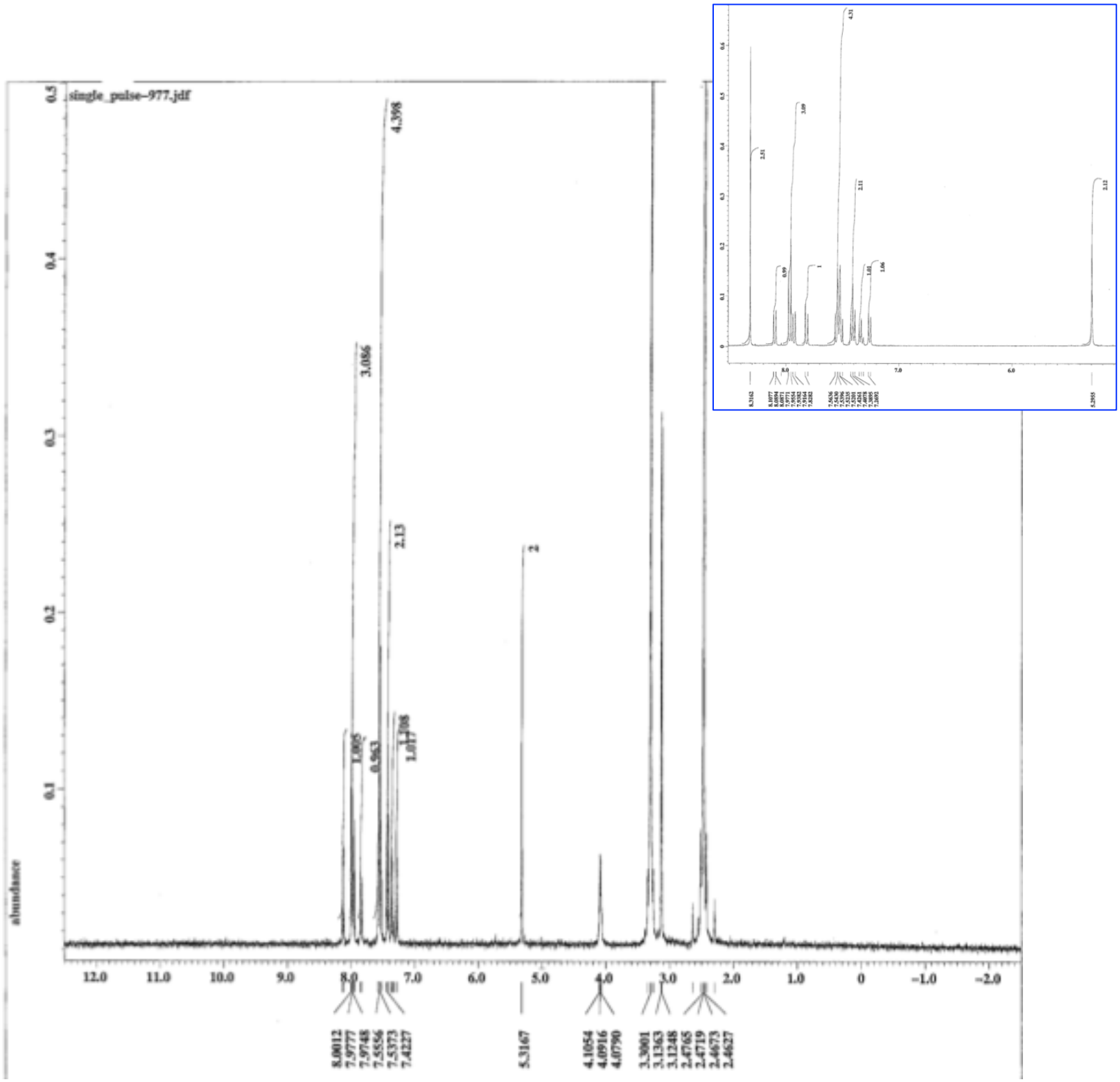

Figure S22. [1]H NMR spectrum of compound **10** in D-6 DMSO; inset shows aromatic region zoomed in. Residual peaks at 4.09 and 3.12 are due to methanol and peaks at 3.30 and 2.47 are due to water and DMSO, respectively. Estimate of purity: 92%.

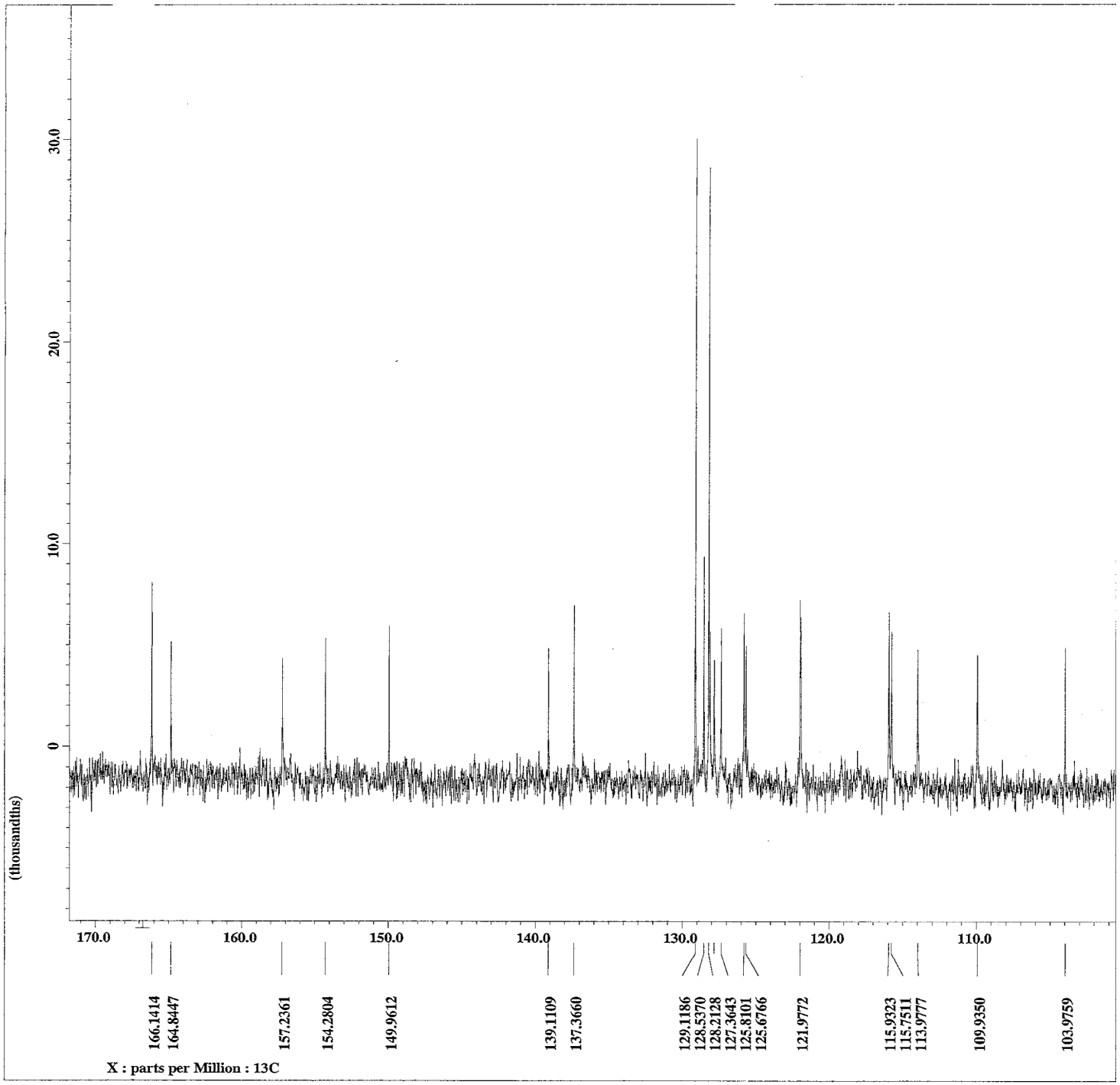

Figure S23. ^{13}C NMR spectrum of compound **10** in D6-DMSO.

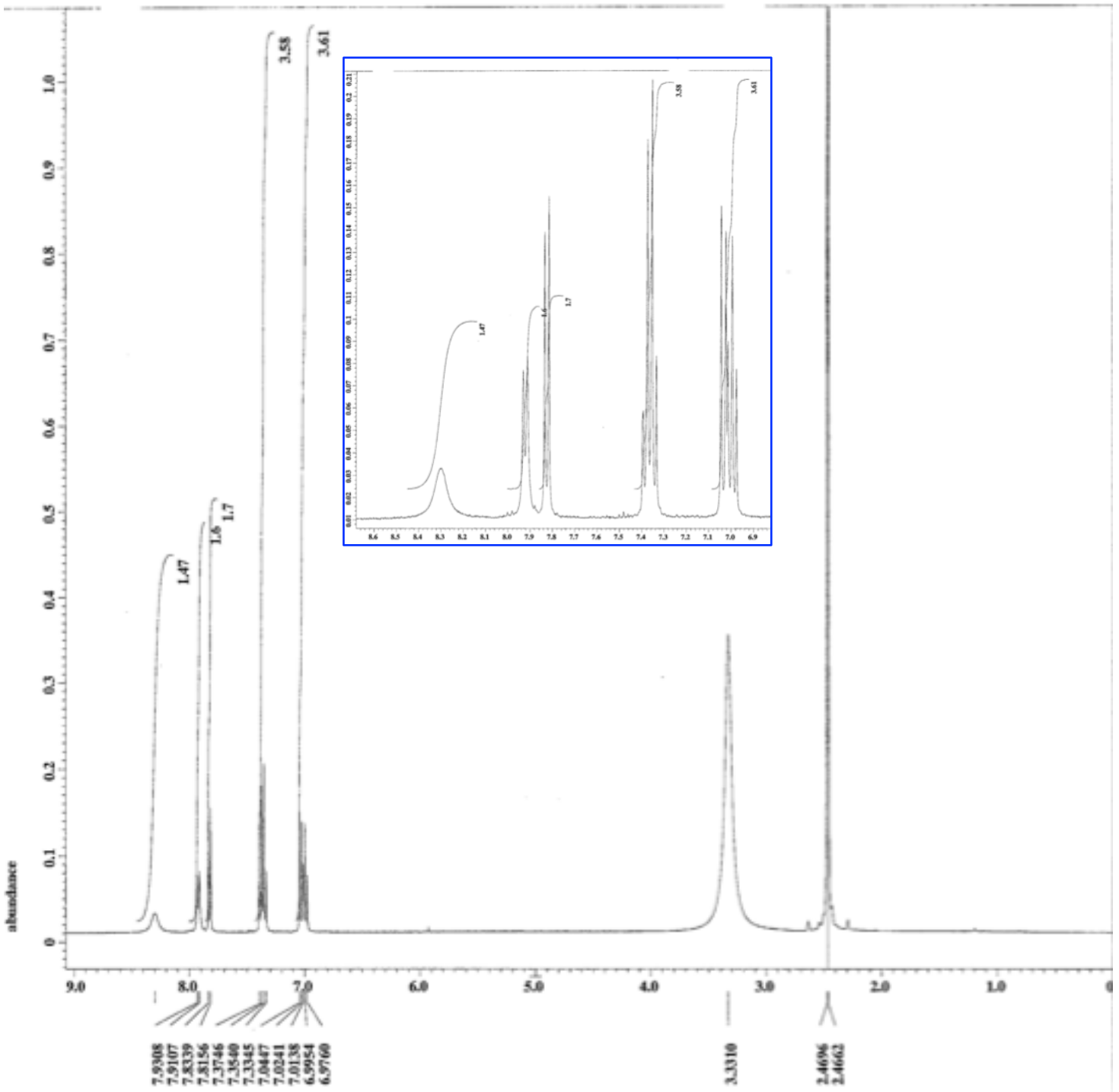

Figure S24. [1]H NMR spectrum of compound **11** in D6-DMSO; inset shows aromatic region zoomed in. Residual peaks at 3.33 and 2.47 are due to water and DMSO, respectively. Estimate of purity: 95%.

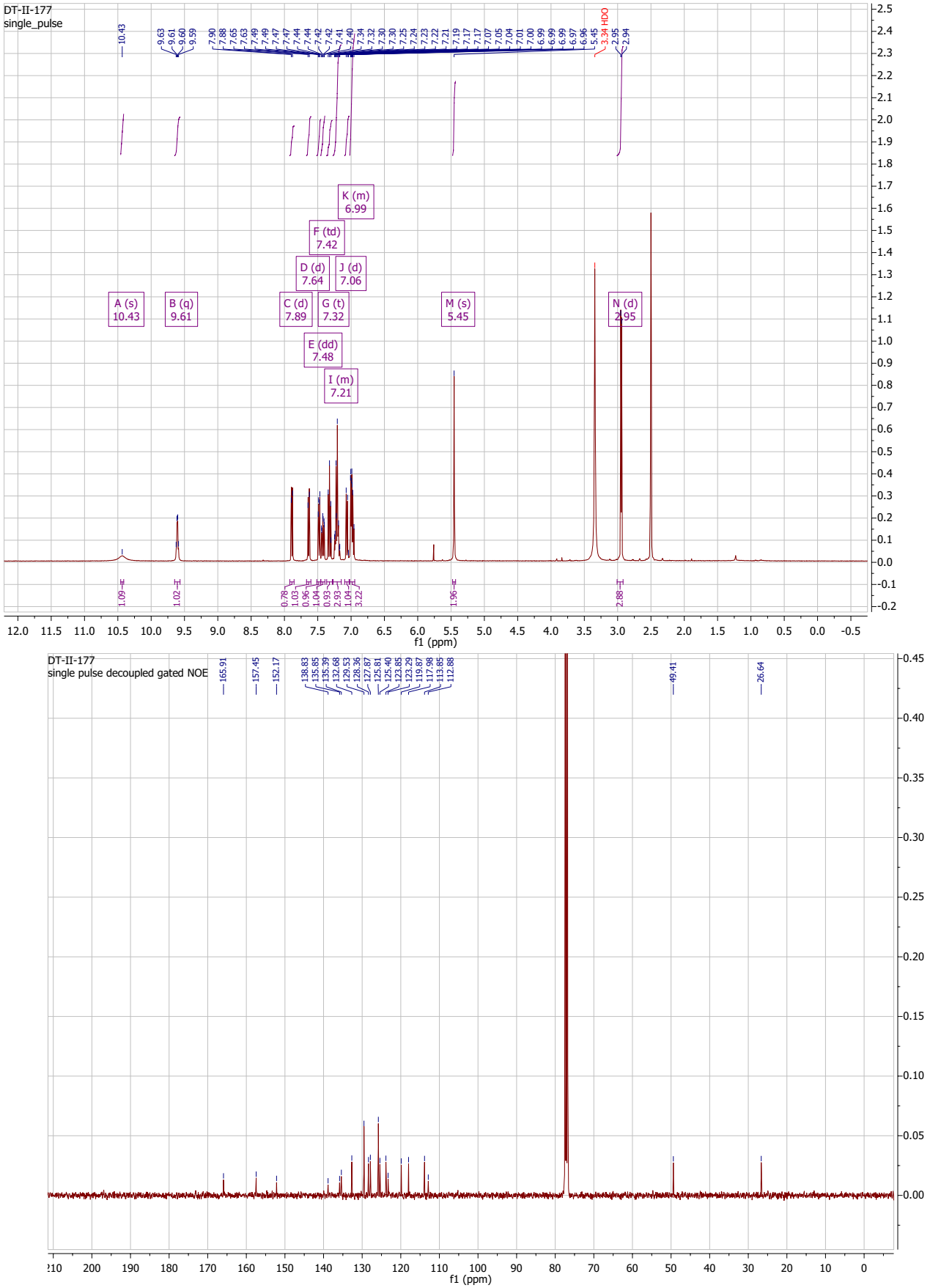

Figure S25. ^{1}H (top) and ^{13}C NMR spectra of compound **12**. The ^{1}H NMR spectrum is in D6-DMSO and residual peaks at 3.33 and 2.47 are due to water and DMSO, respectively; the ^{13}C NMR spectrum is in $CDCl_3$. Estimate of purity: 97%.

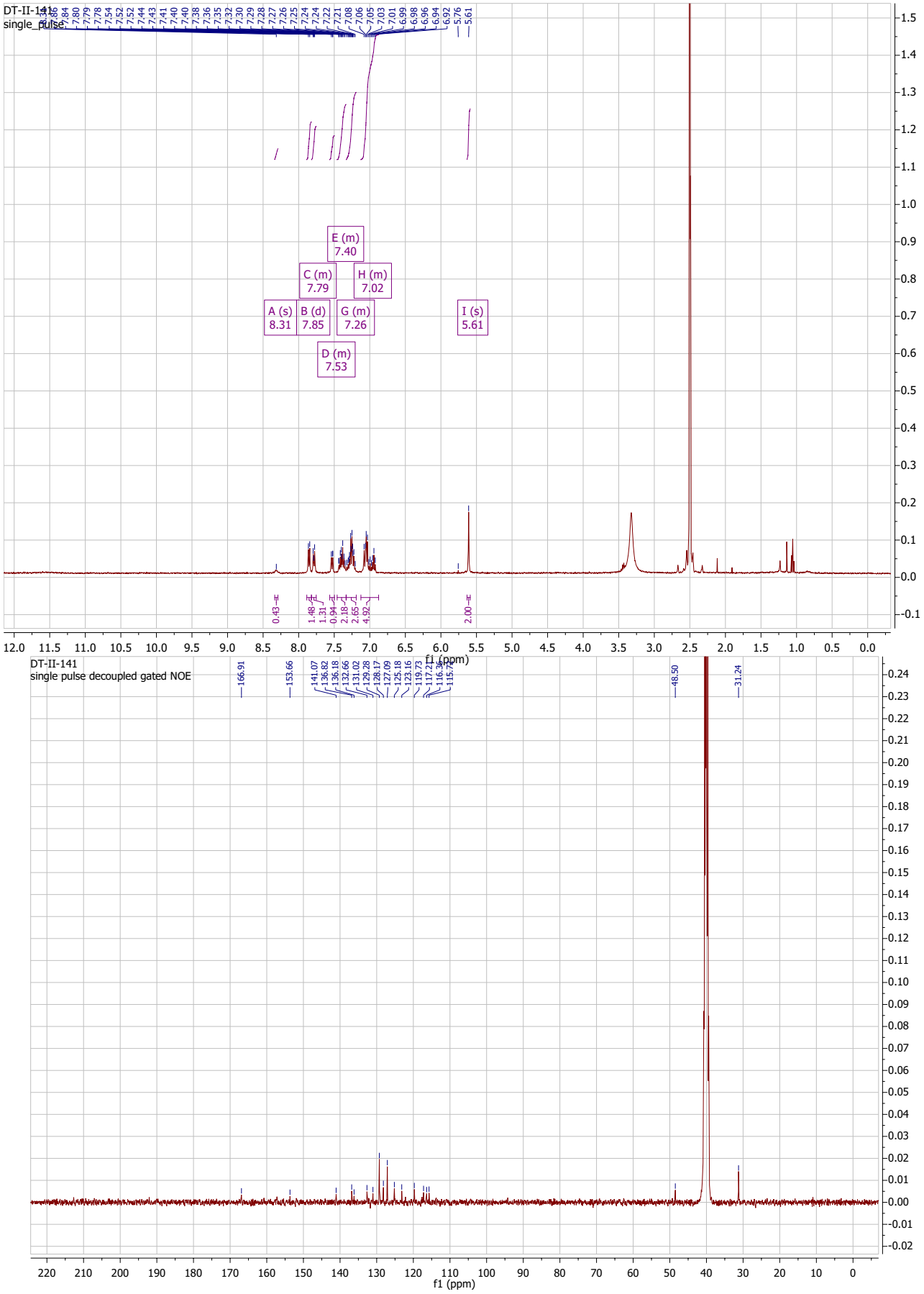

Figure S26. ^{1}H (top) and ^{13}C NMR spectra of compound **13** in D6-DMSO. In the 1H NMR spectrum, residual peaks at 3.44 and 1.06 are due to ethanol and peaks at 3.33 and 2.47 are due to water and DMSO, respectively. Estimate of purity: 95%